

Mixing and Product Distribution with Series-Parallel Reactions in Stirred Tank and Distributed Feed Reactors

B. W. RITCHIE and A. H. TOBGY¹

Department of Chemical Engineering, University of Exeter, Devon, England

Micro- and macromixing models are presented which enable one to correlate the effects of the operating variables with the performance of multistage reactors. Comparison between the single parameter micromixing model and the single parameter models of Ng and Rippin and of Villermaux and Devillon indicate general agreement on micromixing effects for two isothermal series parallel reactions in a CSTR. For distributed feed reactors segregation improves performance for premixed feedstreams and reduces maximum yields for unpremixed feedstreams. Macromixing is characterized by the theoretical and experimental residence time frequency functions of a distributed feed reactor. Analysis of reactor performance shows that, although improvement in maximum yield obtained by using crossflow is small, it is possible to operate at high yields while reducing reactant conversion.

To analyze the importance of mixing on product yield in chemical reactors, many models have been developed. They have concentrated mainly on the effects of residence time and micromixing for single reactions with arbitrary kinetics. With more complex reactions (several products) where high conversion should be accompanied by high selectivity, mixing will probably be more important.

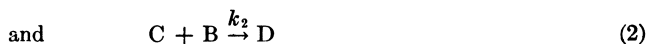
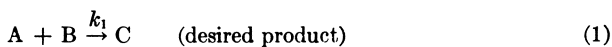
A qualitative analysis by Levenspiel (1) indicates the importance of mixing on product distribution for various complex reactions. For series-parallel reactions various contacting patterns are possible, leading to big differences in product distribution. To consider quantitatively these effects in reactors with distributed feeds such that the residence time distributions of the separate feedstreams are different, the deterministic flow, stochastic micromixing model of Treleaven and Tobgy (2) was invoked. This model was applied to a set of two series-parallel reactions which are assumed to have second-order kinetics

¹ On leave from the Department of Chemical Engineering, University of Cairo, Giza, Cairo, Egypt.

and to take place isothermally with no volume change. The importance of macromixing characterized by the residence time distributions and of micro-mixing characterized by the degree of segregation intermediate between the states of complete segregation and of maximum species and age mixedness (3), on the selectivity, yield, and conversion was determined.

General Considerations

Ideal States of Mixing. The reaction chosen is typical of many important industrial systems, such as the nitration and halogenation of hydrocarbons, the addition reactions of alkenes with proton donors, and the saponification of polyesters, where the intermediate product is desired. These processes are frequently bimolecular, irreversible, and, when occurring in the liquid phase, essentially constant density reactions. The reactions considered are:



where k_1 and k_2 are the reaction velocity constants; selectivity, σ , and yield, η , may be defined with reference to either A or B, such that,

$$\sigma_{CA} = \frac{c_C}{c_{AO} - c_A}; \quad \sigma_{CB} = \frac{c_C}{c_{BO} - c_B}; \quad \eta_{CA} = \frac{c_C}{c_{AO}} = \sigma_{CA}X_A; \quad \eta_{CB} = \frac{c_C}{c_{BO}} = \sigma_{CB}X_B$$

Reaction behavior in plug flow (or batch) reactors, in perfectly mixed continuous stirred tank reactors and in combinations of these reactors, has been considered (1, 4-10). To improve performance, recent publications have considered operating stirred reactors under semicontinuous conditions (11-13) while others have advocated the use of temperature programming (14).

With steady operating conditions in an isothermal reactor, product distribution at different conversions is determined by solving relevant material balances. The ratio of the rate equations of A and C eliminates the time variable so that,

for a plug flow (or batch) system:

$$\frac{\partial c_C}{\partial c_A} = K \left(\frac{c_C}{c_A} \right) - 1 \quad (3)$$

and for a single PCSTR:

$$\frac{c_C}{c_{AO}} = \frac{1 - \frac{c_A}{c_{AO}}}{1 + K \left(\frac{c_{AO}}{c_A} - 1 \right)} \quad (4)$$

Levenspiel (1) indicates product behavior at different conversions of A. For any value of K , selectivity and yield are higher in a PFR than in a single PCSTR. In both cases the yield of the intermediate can pass through a maximum, whose magnitude increases with decreasing K and occurs at increasing conversions. To determine the effects of reactor holding time and initial reactant concentrations, it is necessary to solve the relevant rate equations (6, 7, 8). Their solutions indicate that although any reaction path is determined

Table I. Conditions Necessary for Maximum Yield in Ideal Reactors

| | <i>PFR (or Batch)</i> | <i>1-PCSTR</i> |
|------------------------------|---|--|
| Conversion of A | $X_A = 1 - K^{1/(1-K)}; K \neq 1$ $X_A = 0.632; K = 1$ | $X_A = 1/(1 + K^{1/2})$ |
| Damkohler number | Da_1 is a function of (X_A, K, β) ; the rate equations must be solved simultaneously. | $Da_1 = \frac{1}{K^{1/2} \left[\beta - \frac{2K^{1/2} + 1}{(K^{1/2} + 1)^2} \right]}$ |
| Maximum yield | $\eta_{CA} = K^{K/(1-K)}; K \neq 1$ $\eta_{CA} = 0.368; K = 1$ | $\eta_{CA} = 1/(1 + K^{1/2})^2$ |
| Minimum stoichiometric ratio | $\beta = 2(1 - K^{1/(1-K)}) - K^{K/(1-K)}; K \neq 1$ $\beta = 0.896; K = 1$ | $\beta = \frac{1}{1 + K^{1/2}} \left[2 - \frac{1}{1 + K^{1/2}} \right]$ |

by reactor type and the value of K , the position along the path at any holding time is a function of β and the Damköhler number (Da_1). Decreasing β at fixed Da_1 improves the selectivity. Table I summarizes the conditions necessary for maximum yield in a PFR and single PCSTR. The optimum combination of selectivity and yield at which a reactor operates depends largely on the value of the raw materials and products and the cost of subsequent separation.

Intermediate States of Mixing. If the hydrodynamic properties of the fluids, the reactor geometry, and agitation are such that mixing is not ideal, the relationships on which the reaction paths of a PFR or PCSTR are formulated become invalid. It then is necessary to develop a model which considers mixing effects. The most successful approach used to characterize intermediate states of mixing seems to be that involving the random coalescence model involving a single mixing history parameter, I , and simulated by Monte Carlo methods. Other approaches have been used to establish whether micromixing affects the outcome of various reactions by quantifying the difference between the extreme mixedness states of complete segregation and maximum mixedness (15). Tobgy (16) has reviewed this subject in great detail.

For I to be an essentially hydrodynamic parameter it should be independent of those parameters which characterize the chemical reactions; for isothermal homogeneous second-order reactions, these are the first Damköhler number and the stoichiometric ratio. The jet reactor mentioned below and described by Treleaven and Tobgy (17) was designed as a relatively severe experimental test of whether I is such a suitable hydrodynamic parameter, and this was shown to be the case. There is however no inherent reason in formulating random coalescence models for using a single value of I to characterize micromixing throughout a given reactor. In correlating the experimental data of Vassilatos and Toor (18) for an unpremixed feed tubular reactor, Kattan and Adler (19) found that the model that closely fitted the results involved a variation of I with axial position. On the other hand, others (20, 21, 22, 23) have correlated the same data using two different models, each based on single values of I , and I was independent of the chemical reaction parameters above. Evangelista *et al.* (24) showed that for a given working fluid in stirred tanks of similar geometric dimensions, the theory of homogeneous, isotropic turbulence leads to a value of I which agrees well with the experimental results for the overall mixing time determined by Van de Vusse (25). A similar approach was adopted by Otte *et al.* (26). Evangelista *et al.* (27) also used a single value of I and turbulence theory to analyze the effect

of imperfect mixing on stirred combustion reactors. Komasaawa *et al.* (28) and Villermaux and Devillon (29) studied second-order and complex reactions in two-phase continuous flow stirred tanks and obtained good agreement, within experimental error, between coalescence and redispersion rate as determined by chemical conversion and direct physical measurements. The foregoing seems to suggest that I does account for the fluid mixing patterns within the vessel and is independent of the reaction—providing the reacting fluids have the same hydrodynamic characteristics.

The Random Coalescence Model

Formulation. The flow process is simulated in a non-random manner by using deterministic forms of the residence time frequency functions (2). Each residence time and residual lifetime frequency function is expressed in K_λ discrete intervals of magnitude $\Delta\lambda$. Elements from the K_λ th residence time interval of each feedstream are entered into the K_λ th residual lifetime interval in the reactor, and on the basis of the value of I , a corresponding number of elements are selected at random, and instantaneous pairwise coalescence and redispersion simulate the micromixing. I is the average number of coalescences and redispersions experienced by each fluid element in the reactor. After these flow and micromixing steps, the batch kinetics are integrated over the residual lifetime interval, $\Delta\lambda$, for each fluid element. These three simulation steps are repeated for each decreasing residual lifetime interval until $\lambda = 0$, when all elements with zero residual lifetime exit the reactor. The selectivity and yield of the desired product and the conversions of the reactants are calculated from the population of leaving elements.

Integrating the Batch Kinetics. At the end of each flow and micromixing step in the simulation procedure, each fluid element is subjected to a batch reaction of duration $\Delta\lambda$. The number of reaction rate equations to be solved can be reduced from four to two by defining conversion parameters, v and w so that the concentrations of the reacting species are:

$$\bar{c}_A = \bar{c}_{AO} - \bar{v}; \bar{c}_B = \bar{c}_{BO} - \bar{v} - \bar{w}; \bar{c}_C = \bar{v} - \bar{w}; \text{ and } \bar{c}_D = \bar{w}.$$

Material balances on reactant A and product D then give:

$$\frac{d\bar{v}}{dt} = k_1 (\bar{c}_{AO} - \bar{v}) (\bar{c}_{BO} - \bar{v} - \bar{w}) \quad (5)$$

and,

$$\frac{d\bar{w}}{dt} = k_2 (\bar{v} - \bar{w}) (\bar{c}_{BO} - \bar{v} - \bar{w}) \quad (6)$$

where

$$\bar{c}_{AO} = \bar{c}_A + \bar{c}_C + \bar{c}_D \quad (7)$$

and,

$$\bar{c}_{BO} = \bar{c}_B + \bar{c}_C + 2\bar{c}_D \quad (8)$$

Further treatment of the parent rate equations reduces the number of differential equations to one:

$$\frac{d\bar{c}_A}{dt} = -k_1 \left[\left(\frac{1-2K}{1-K} \right) \bar{c}_A + \left(\frac{\bar{c}_{AO}^{1-K}}{1-K} \right) \bar{c}_A^K - \bar{c}_O \right] \bar{c}_A; K \neq 1 \quad (9)$$

where

$$\bar{c}_O = 2\bar{c}_{AO} - \bar{c}_{BO} \quad (10)$$

Solution of Equation 9 gives $c_A(t)$, and the concentration of B can be calculated from

$$\bar{c}_B = \left(\frac{1 - 2K}{1 - K} \right) \bar{c}_A + \left(\frac{c_{AO}^{1-K}}{1 - K} \right) \bar{c}_A^K - \bar{c}_0; K \neq 1 \quad (11)$$

The concentration of C and D follow from a material balance

$$\bar{c}_C = \bar{c}_B - 2\bar{c}_A + \bar{c}_0 \quad (12)$$

$$\bar{c}_D = \bar{c}_A - \bar{c}_{AO} - \bar{c}_B + \bar{c}_{BO} \quad (13)$$

Here, the batch kinetics were integrated using a sixth-order Runge-Kutta procedure (30). The integration time step length is given by

$$Dt_{RK} = \Delta\lambda / \text{DENOM} \quad (14)$$

where DENOM is an integer input to the simulation procedure. With high values of Da_1 it was necessary to specify a large value for DENOM (*e.g.*, with $Da_1 = 100$ and $\beta = 0.5$, Dt_{RK} was $\tau/800$). In attempting many simulations in this region it would help to use predictor-corrector techniques (31) to solve the differential equations. In solving the set of batch kinetic equations, generally no computer time was saved in reducing the differential equations to one.

Simulations. Simulations were done on an ICL 4/50 computer using a total feed population of $M = 200$ elements. The residence time and residual lifetime distributions were discretized into intervals of *ca.* $\tau/40$ sec. The number of elements representing the reactor population follows from $N_R = M\tau/\Delta\lambda$. In calculating Da_1 and the stoichiometric ratio, the flow weighted inlet concentrations were calculated from

$$c_{AO} = \frac{\sum_{j=1}^2 Q_j c_{Aj0}}{\sum_{j=1}^2 Q_j}, \quad c_{BO} = \frac{\sum_{j=1}^2 Q_j c_{Bj0}}{\sum_{j=1}^2 Q_j} \quad (15) \text{ and } (16)$$

where c_{Aj0} and c_{Bj0} are the inlet concentrations of A and B, respectively, in stream j .

Checking the Simulation Algorithms. To test the simulation procedure and the associated computer programs, initial trials were done using the residence time frequency function of a single CSTR to characterize macromixing. In these cases,

$$f_1(t) = f_2(t) = \left(\frac{1}{\tau} \right) e^{-t/\tau} \quad (17)$$

Both premixed and unpremixed feed stream situations were considered, and K , Da_1 , and β were selected to allow comparison between the predictions of the random coalescence model and those of the single parameter models of Villermoux and Devillon (29) and of Ng and Rippin (32), as applied by Anand (33).

COMPARISON WITH THE MODEL OF VILLERMAUX AND DEVILLON. In quantifying the effects of micromixing in 1-CSTR, Villermoux and Devillon (29) assumed a particular coalescence and redispersion mechanism and defined a transfer coefficient such that the concentration of an element within the reactor

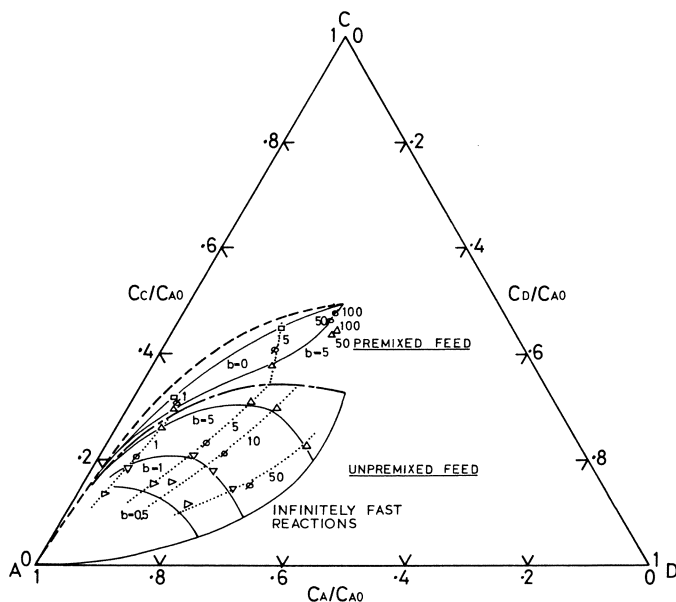


Figure 1. Comparison with the predictions of Villermaux and Devillon's model, when $K = 0.5$, $\beta = 1$. Random coalescence model: \square , $I = 0$; Δ , $I = 2$; ∇ , $I = 4$; ϕ , $I = 5$; \triangle , $I = 20$; —, data of Villermaux and Devillon (29); — — —, PFR; · · · · ·, 1-PCSTR; · · · · ·, lines of constant Damköhler number.

population evolves as a function of time:

$$\frac{dc_i}{dt} = h(\bar{c}_i - \bar{c}_i) - r_i, \quad i = A, B, C, D \quad (18)$$

where \bar{c}_i is the average concentration of coalescing elements. The fluid interaction mechanism is that postulated by others (34, 35, 36). Villermaux and Devillon related the transfer coefficient, h , to the frequency of coalescence, ω , by

$$h = \omega/4 \quad (19)$$

and introduced a dimensionless micromixing parameter $b (= h\tau)$ such that when $b = 0$, the reactor is completely segregated, and when $b = \infty$, the reactor is at maximum mixedness.

Figure 1 shows the results of simulations with $K = 0.5$, $\beta = 1$, and $1 \leq Da_1 \leq 100$. Maximum mixedness conversions are calculated from the material balance equations for a single PCSTR. Solid lines are predictions of reactor performance based on the Villermaux and Devillon model for premixed and unpremixed feedstreams; also shown are the predicted average exit concentrations based on the random coalescence model and premixed PFR. Two distinct regions are formed, depending on whether the feed is premixed or unpremixed. Serious quantitative comparison between the models is difficult for premixed feedstreams because micromixing effects are small; the models do however predict behavior within the same limits. Conversions calculated

with intermediate mixing are bounded by the completely segregated and maximum mixedness conversions. Segregation favors both selectivity and yield. With high Da_1 values and finite values of the micromixing parameters both models indicate that behavior is approaching that in a PFR; only in the maximum mixedness case does the reaction path terminate at the maximum mixedness conversion. This is understandable because since Da_1 is high, conversions are calculated with high values of k_1 and k_2 resulting in reactant B being almost entirely consumed in the fluid elements before the latter have had time to coalesce or to exit from the reactor.

With unpremixed feedstreams, conversion with intermediate mixing states fall between the maximum mixedness conversion and that calculated on the basis that the reactions are infinitely fast (*i.e.*, k_1 and k_2 are very large, but the ratio K remains constant). Here segregation is detrimental to performance. Although the two models are based on different mechanisms of fluid element interaction and thus do not compare exactly in their predictions, these predictions are not very different if $I = 4b$, at least where interaction is significant, $0 < I < 40$. Only when segregation is high and the concept of an average concentration influencing the rate of transfer becomes less than realistic do the models' predictions differ considerably ($I < 4$, $b < 1$). Under such conditions, the random coalescence model would be expected to represent local conditions better (37).

COMPARISON WITH THE MODEL OF NG AND RIPPIN. The micromixing model of Ng and Rippin (32) stipulates an entering environment which is in a state of complete segregation and a leaving environment which is in a state of maximum mixedness. The exit stream from the reactor is a mixture from both environments, and it is assumed that any fluid element in the entering environment has an equal probability of being transferred to the leaving environment. The rate of transfer between these two environments is

$$-\frac{dm}{dt} = mR \quad (20)$$

For second-order and autocatalytic reactions in a single CSTR, Tobgy (38) has shown that if a reduced yield, Y , is defined such that $Y = \text{actual yield}/\text{yield at maximum mixedness}$, a unique relationship exists between Y and the micromixing parameter, $R\tau$,

$$Y = \frac{R\tau}{R\tau + 1} \quad (21)$$

which is not a function of any reaction parameter excepting as they influence the maximum mixedness conversion. On analyzing the results of Anand (33). Equation 21 was found also to hold for series-parallel reactions (Figure 2).

The models are identical in their predictions for reactors at maximum mixedness; transfer between the entering and leaving environments is complete. Intermediate mixedness represented by the Ng and Rippin model is defined in terms of elements in the two extreme states only; this is not the case with the random coalescence model, and a reactor operating with an arbitrary state of micromixing may contain elements having a spectrum of mixing states. Nevertheless, both models indicate micromixing effects of the same order of magnitude, but with the random coalescence model the relationship between Y and I is not unique. The random coalescence model presented here, when applied to 1-CSTR, should give results identical to the model of Spielman and Levenspiel (39) and Kattan and Adler (40) since the micromixing mechanism

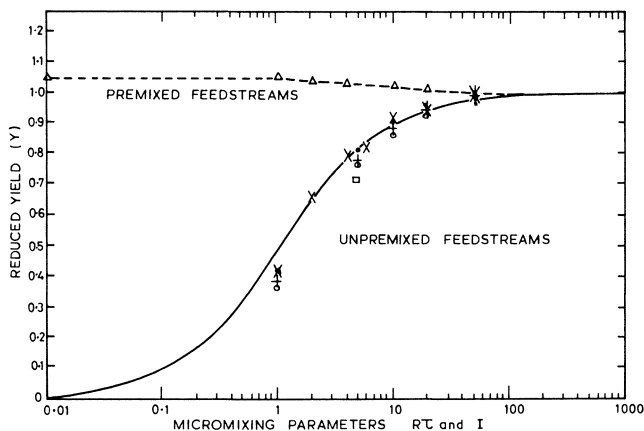


Figure 2. Comparison with the predictions of Ng and Rippin's model. Random coalescence model (Y vs. I).

| | β | K | Da_1 |
|---|---------|---|--------|
| ○ | 1 | 3 | 0.544 |
| + | 1 | 5 | 0.544 |
| △ | 3 | 3 | 0.198 |
| ● | 3 | 3 | 0.544 |
| □ | 3 | 5 | 0.138 |
| × | 3 | 5 | 0.544 |

—, $R\tau/(R\tau + 1)$ vs. $R\tau$ and also Y vs. $R\tau$ based on the results of Anand (33).

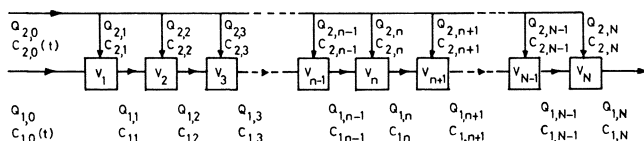


Figure 3. Multistage reactor with fresh feed introduction between stages

is the same. Rao and Edwards (41) have indicated general agreement between the Ng and Rippin model and that of Spielman and Levenspiel.

Performance in Reactors with Feed Distribution

To improve selectivity reactant A should react uniformly while reactant B should be introduced so that the concentration of A is kept high and that of B is kept low. To do this, one can operate stirred reactors semicontinuously by adding B gradually into a vessel which already contains all of feed A (11, 12). For continuous reactors a crossflow system such as that in Figure 3 can be used. In such a system each feedstream has its own residence time distribution.

Effects of Micromixing. To predict the effects of micromixing in reactors with distributed feed, one set of experimentally determined residence time distributions for the axisymmetric jet reactor (42) was used to characterize macromixing. Stream 2 is the jet stream, and stream 1 is the surrounding

secondary flow. The different residence time distributions for the streams were produced by using a relatively high U_2/U_1 , and turbulent entrainment was achieved by keeping the jet Reynolds' number above 1500. Figure 4 shows the values of the flow rates, mean residence times, and residual lifetime frequency functions. The residence time frequency functions are available (42). Analysis of these residual lifetime distributions indicates that only elements of stream 1 are available for micromixing at $\infty < \lambda < 11$. Population balances on the elements forming the reactor population show that this region accounts for 8% of the reactor volume. At $11 < \lambda < 4$, which accounts for 42% of the reactor volume, stream 1 is in excess volumetrically, and selectivity should be highest when the reactants are introduced separately and stream 2 contains reactant B.

Reactor performance has been simulated at $0.05 < K < 10$, for industrially important series-parallel reactions (4, 9). In particular, consideration is given to the effects of mixing intensity (I), Da_1 , and the method of introducing the feedstreams on the selectivity and yield of the intermediate product when the residual lifetime distributions of Figure 4 characterize the macromixing.

Three methods for introducing the reactants are considered. Two are for unpremixed feedstreams and arise when stream 2 contains only A and then only B; the third is for premixed feedstreams both containing A and B. Initial simulations were done with $\beta = 1$ and $K = 1$ at $0 < Da_1 \leq 10$, with two values of I :

(a) $I = 7.5$, a typical value found (17) on calibrating the reactor using a known second-order reaction

(b) $I = 100$ which would correspond to micromixing conditions in a distributed feed reactor operating at almost maximum mixedness.

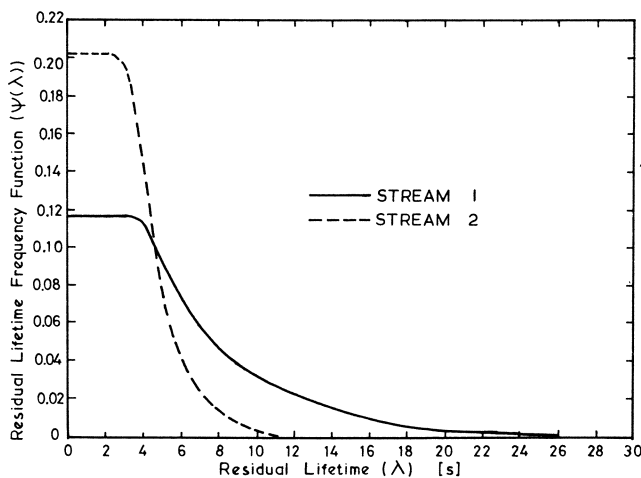


Figure 4. Residual lifetime frequency functions for the jet reactor. —, coaxial secondary stream; $Q_1 = 50 \text{ cm}^3 \text{ sec}^{-1}$; $\tau_1 = 8.52 \text{ sec}$. ----, central jet stream; $Q_2 = 50 \text{ cm}^3 \text{ sec}^{-1}$; $\tau_2 = 4.94 \text{ sec}$.

The results in Figure 5 indicate that the method can be influenced largely by the degree of segregation in the reactor and that performance, even with low mixing intensities, is generally better than operation in 1-PCSTR. For the

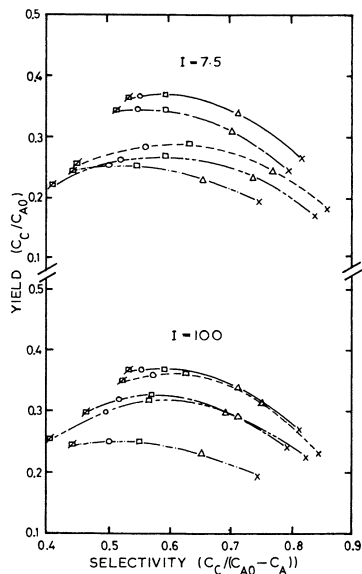


Figure 5. Yield vs. selectivity with jet reactor RTD's, at two values of I and three operating policies vs. a PFR and single PCSTR; $K = 1$; $\beta = 1$.

————, PFR; ————, 1-PCSTR;
 - - - -, jet reactor with stream 1 containing only B and stream 2 containing only A
 - · - · -, jet reactor with stream 1 containing only A and stream 2 containing only B
 — · — · —, jet reactor with both streams containing premixed A and B.
 ×, $Da_1 = 0.5$; Δ , $Da_1 = 1$; \square , $Da_1 = 2.43$;
 \circ , $Da_1 = 4$; \diamond , $Da_1 = 10$.

jet reactor and $I = 7.5$, conditions are segregated, and the highest yields occur when the feedstreams are premixed; selectivities approach those obtainable with plug flow, although the yields are lower.

When the reactants are introduced separately, selectivity and yield (at the same Da_1) are higher when B is introduced in the stream with the shorter mean residence time—i.e., stream 2. When Da_1 is less than the plug flow optimum of 2.43, selectivities with separate feeding are greater than those with plug flow, but the yield is reduced. With $I = 100$ and stream 2 containing only B, the reaction path closely matches that with plug flow, and selectivity is markedly improved for $Da_1 < 2.43$. Figure 5 also shows that the yield increases with Da_1 and passes through a maximum at or near the plug flow optimum. In each case, however, the maximum yield is lower.

Figure 6 shows the effect of changing I on the selectivity and yield for three values of K . With these reaction conditions, selectivities are relatively insensitive to micromixing; only at low K is increased mixing intensity accompanied by increased selectivity. In all cases, however, increased mixing intensity

is accompanied by an increased yield and conversion as more of the reactor volume becomes effective.

The dependence of the yield from the jet reactor on the reaction velocity constant ratio is shown in Figure 7. The yields for plug flow operation, and steady state processing in a single PCSTR are the maxima obtainable with these

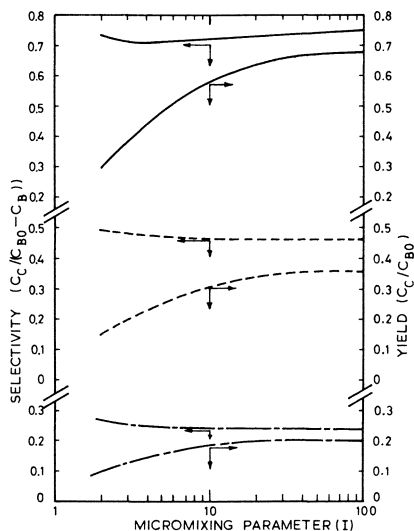


Figure 6. Effect of micromixing on selectivity and yield when jet reactor is operated with stream 1 containing only A, and stream 2 containing only B.

| | K | β | Da_1 |
|-------|-----|---------|--------|
| — | 0.1 | 1.127 | 11 |
| - - - | 1 | 1 | 2.43 |
| - - - | 8 | 0.443 | 2 |

K ratios. In each case β was chosen so that the PFR and PCSTR would operate with 95% conversion of B:

$$\beta = \frac{2X_A - \eta_{CA}}{0.95} \quad (22)$$

where X_A and η_{CA} are calculated from Table I, and Da_1 is calculated accordingly. The jet reactor was considered to operate with the same Da_1 and β as calculated for plug flow operation and with stream 2 containing only B. The highest yield at each K is that from plug flow operation, but with the segregated jet reactor ($I = 7.5$) the yield is greater than that from a single PCSTR when $K > 1.5$, and the selectivity is greater than that obtainable with plug flow. For example, when $K = 1$, the jet reactor yield is 3% less than that from the PCSTR, but selectivity is 29% greater; when $K = 8$, the jet reactor yield is 19% greater than the PCSTR's, and selectivity increases by 64%. Since the calculations are based on a PFR and single PCSTR operating at the same conversion of B, the volume requirement of the jet reactor would be considerably less than its PCSTR counterpart.

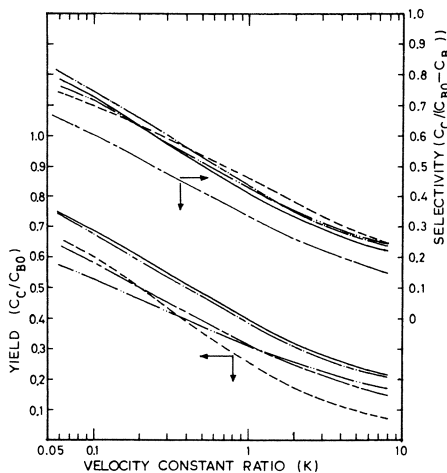


Figure 7. Selectivity and yield obtainable with jet RTD's vs. steady-state processing in a PFR, a single PCSTR, and with unsteady processing in a single PCSTR (13) as a function of the velocity constant ratio. — · — · —, jet reactor with $I = 100$; — · — · —, jet reactor with $I = 7.5$; — — —, PFR; — — — —, steady PCSTR; - - - - -, pulsed PCSTR.

The selectivities and yields possible with periodic operation of a PCSTR (13) are included in Figure 7. They were calculated at the optimum period θ and with $\beta = 1$ at each K value. While the jet reactor is better than a PCSTR when $K > 1.5$, at the other end of the scale ($K < 0.2$) periodic operation offers a similar improvement, but the volume requirement of the reactor is not reduced.

Effects of Macromixing. In illustrating the effects of micromixing, consideration has been restricted to the effects of changing the intensity of mixing for a single macromixed state. One feature of series-parallel reactions is the variety of contacting patterns possible. To consider the effects of such changes on the maximum mixedness conversions, the authors have developed a model for the residence time distributions in general multistage systems with fresh feed introduction between stages (43).

A schematic of the system is shown in Figure 3, and the residence time frequency functions, when each stage is a perfect macromixer are:

$$f_1(t) = \sum_{j=1}^N \frac{\frac{N}{\pi} \left(\frac{1}{\tau_i} \right) e^{-t/\tau_j}}{\sum_{\substack{i=1 \\ i \neq j}}^N \frac{N}{\pi} \left(\frac{1}{\tau_i} - \frac{1}{\tau_j} \right)} \quad (23)$$

$$f_2(t) = \left(\frac{1}{\tau_N Q_{2,0}} \right) \sum_{k=1}^N \sum_{j=N+1-k}^N \frac{Q_{2,N+1-k} \frac{N-1}{\pi} \left(\frac{1}{\tau_i} \right) e^{-t/\tau_j}}{\sum_{\substack{i=N+1-k \\ i \neq j}}^N \frac{N}{\pi} \left(\frac{1}{\tau_i} - \frac{1}{\tau_j} \right)} \quad (24)$$

where $\tau_j = \frac{V_j}{Q_{i,j}}$, $j = 1, 2 \dots N$, and all τ_j are different. (25)

To show the effects of changing the feed distribution, results are reported for a system where stream 2 is distributed so that the cross-flow forms an arithmetic progression, so that:

in general,

$$Q_{2,n} = Q_{2,n-1} + d_Q \quad (26)$$

and, in particular,

$$Q_{2,n} = \frac{Q_{2,n}}{N} - \frac{1}{2} (N + 1) d_Q + n d_Q \quad (27)$$

and

$$Q_{1,n} = Q_{1,0} + n \left[\frac{Q_{2,0}}{N} - \frac{1}{2} (N + 1) d_Q \right] + \frac{n(n+1)}{2} d_Q \quad (28)$$

When each stage in the cascade is a PCSTR, the conversion can be calculated by applying steady-state material balances across each stage in turn. Such a reactor is in the state of sequential mixedness (44). To illustrate the possible operating policies available for a series of equal volume PCSTR's, results are

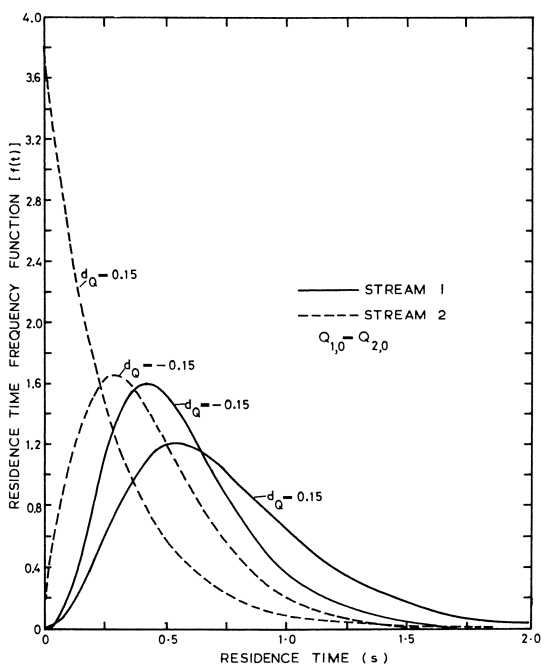


Figure 8. Residence time frequency functions of four PCSTR's in series with crossflow of stream 2 between stages. $V/(Q_{1,0} + Q_{2,0}) = 0.5$ sec.

reported for a four-stage cascade. In order that each $Q_{2,n}/Q_{2,0}$ is always greater than zero, the common difference d_Q must be:

$$-\frac{2}{N(N-1)} < \frac{d_Q}{Q_{2,0}} < \frac{2}{N(N-1)} \quad (29)$$

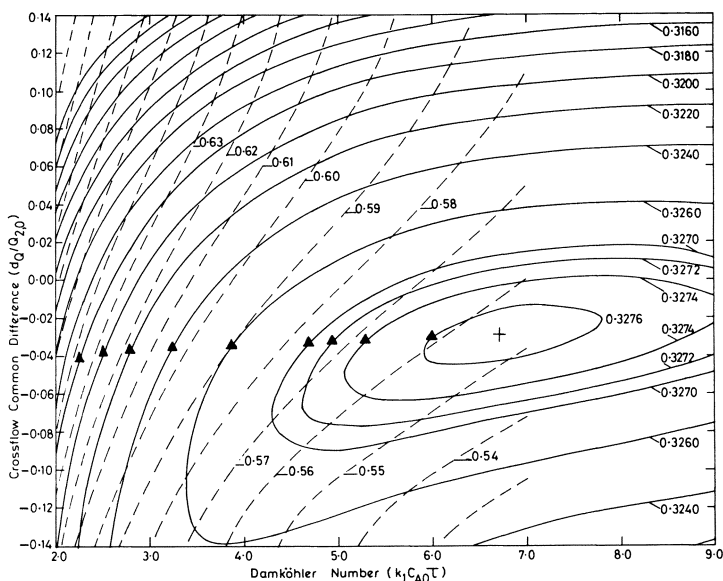


Figure 9. Yield and selectivity of an equal-volume, four-stage reactor in the state of sequential mixedness as a function of $d_Q/Q_{2,0}$ and Da_1 . \blacktriangle Conditions for high yield accompanied by high selectivity. ——— Yield of $C(C_c/C_{A0})$. - - - Selectivity $(C_c/C_{A0} - C_A)$.

Thus, in the case in question, $-0.1666 < d_Q/Q_{2,0} < 0.1666$.

Figure 8 shows the residence time frequency functions of the feedstreams when $d_Q = -0.15$ and $d_Q = 0.15$. Stream 2 has a smaller mean residence time than stream 1; as d_Q increases, the mean and variance of the residence time frequency function of stream 1 increases while the mean residence time of stream 2 decreases.

The response surfaces of yield and selectivity as a function of $d_Q/Q_{2,0}$ and Da_1 are shown in Figure 9 when B is the crossflow, stream 1 contains A, $K = 1$, and $\beta = 1$. The maximum yield $(\eta_{CA})_{\max} = 0.3276$ and occurs when $d_Q/Q_{2,0} = -0.029$ and $Da_1 = 6.724$. It represents a 1.7% increase *vs.* that from a four-stage, equal-volume, cascade with no crossflow. Since both reactions are of the same order with respect to B, the improvement in yield when B is distributed across the cascade is small and requires an increase in the total reactor volume for the same production rate. However, Figure 9 indicates that the crossflow cascade can be operated at the maximum yield of a four-stage, equal-volume cascade operated with no crossflow while reducing the conversion of A by about 6.8%.

Discussion

This study was done first to develop a method to predict the performance of multistage distributed feed reactors with fresh feed addition between stages.

Where the stage boundaries are not clearly defined, the conversion limits lie between those of complete segregation and maximum mixedness, based on the exit residence time distributions of each feedstream. Intermediate mixing states can be characterized by the random coalescence model. When the stage boundaries are well defined (*—e.g.*, in a series of stirred tanks with crossflow), sequential application of the random coalescence model can be used to determine performance.

The second objective was to determine whether deviations from ideal mixing are detrimental to reactors with series-parallel reactions. In the cases considered here a degree of segregation will improve performance if the feedstreams are premixed whereas with unpremixed feedstreams, segregation reduces possible maximum yields. An important stage in designing feed distribution systems will thus involve methods of improving micromixing by improving both the design of impellers and method of feed introduction. For example, multiple impellers with multiple feed entry points per impeller could increase micromixing without increasing energy consumption. This need for proper design will become increasingly important as the relative rates of reaction increase, to prevent oversubstitution in segregated regions adjacent to the feed entry points (11).

With the same total reactor volume and with distributed feeding the highest selectivity occurs when B is introduced with the shorter mean residence time. By progressively increasing the crossflow volumetric flow rate across the cascade, the ratio of the mean residence time of stream 2 to stream 1 is reduced; this improves selectivity further, and, with suitable choice of an operating Da_1 number, the sequential mixedness yield can exceed that for a staged reactor with no crossflow.

The best operating conditions for distributed feed reactors are difficult to select because the secondary stream volumetric flow rate and/or the stage volume distribution may be varied. The macromixing models presented here and elsewhere (43) allow direct search algorithms to be applied to optimization of suitably formulated objective functions. Application of the random coalescence micromixing model to these optimum cascades will then indicate quantitatively the micromixing effects and how rapidly performance might be expected to fall off if mixing conditions in the cascade deviate from the ideal.

Nomenclature

| | |
|-------------|---|
| A, B, C, D | reactants |
| b | micromixing parameter of Villermaux and Devillon |
| c | concentration, moles/vol |
| CSTR | continuous stirred tank reactor |
| d_Q | common difference in the crossflow volumetric flow rate, vol/time |
| Da_1 | Damköhler number ($k_1 c_{A0} \tau$) |
| DENOM | integer input to simulation procedure (defined in text) |
| Dt_{RK} | integration time step length |
| f | residence time frequency function, time^{-1} |
| h | transfer coefficient defined by Equation 18, time^{-1} |
| I | micromixing parameter of random coalescence model |
| k | second-order reaction velocity constant, vol/mole/time |
| K | ratio of reaction velocity constants, (k_2/k_1) |
| K_λ | residual lifetime and residence time intervals |
| m | mass of material in the entering environment of the Ng and Rippin model |

| | |
|-------|--|
| M | number of elements representing total feedstream population, dimensionless |
| n | number of a general stage in multistage reactor |
| N | total number of stages in multistage reactor |
| N_R | total number of elements representing reactor population |
| PCSTR | perfectly mixed continuous stirred tank reactor |
| PFR | plug flow reactor |
| Q | volumetric flow rate, vol/time |
| r | rate of reaction, moles/vol/time |
| R | mixing transfer coefficient, defined by Equation 20, time ⁻¹ |
| RTD | residence time distribution |
| t | time, or residence time |
| U | velocity, length/time |
| v | conversion parameter, moles/vol |
| V | reactor volume |
| w | conversion parameter, moles/vol |
| X | fractional molar conversion $[(c_0 - c)/c_0]$ |
| Y | reduced yield (actual yield/maximum mixedness yield) |

Greek symbols

| | |
|-----------|--|
| β | stoichiometric ratio (c_{B0}/c_{A0}) |
| η | yield |
| θ | duration of pulse, defined by Renken (13) |
| λ | residual lifetime |
| σ | selectivity |
| τ | mean residence time |
| ψ | residual lifetime frequency function, time |
| ω | frequency of coalescence, time ⁻¹ |

Subscripts

| | |
|----------------|---|
| o | initial value |
| 1, 2 | streams 1 or 2 or Reaction 1 or 2 |
| A, B, C, D | reactant A, B, C, or D |
| i, j | i th or j th stream or species for the multistage system. For volumetric flowrates and concentrations, i , is feedstream. For stream 2 flows and concentrations, j is the stage into which the material flows. For stream 1 flows and concentrations j is the stage from which the material originates. |
| n | a general stage |
| N | the final stage |
| overbar | fluid element local mean value |
| double overbar | ensemble average of coalescing fluid elements |

Literature Cited

1. Levenspiel, O., "Chemical Reaction Engineering," 2nd ed., Chap. 7, Wiley, New York, 1972.
2. Treleaven, C. R., Tobgy, A. H., *Chem. Eng. Sci.* (1972) **27**, 1497, 1756.
3. Treleaven, C. R., Tobgy, A. H., *Chem. Eng. Sci.* (1971) **26**, 1259
4. Russell, T. W. F., Buzzelli, D. T., *Ind. Eng. Chem., Process Design Develop.* (1969) **8**, 2.
5. Kramers, H., Westerterp, K. R., "Elements of Chemical Reactor Design and Operation," pp. 36-52, Chapman Hall, London, 1963.
6. Kerber, R., Gestrich, W., *Chem. Ing. Tech.* (1966) **38**, 536.

7. Kerber, R., Gestrich, W., *Chem. Ing. Tech.* (1967) **39**, 458.
8. Kerber, R., Gestrich, W., *Chem. Ing. Tech.* (1968) **40**, 129.
9. Friedman, M. H., White, R. R., *AIChE J.* (1962) **8**, 581.
10. Trambouze, P. T., Piret, E. L., *AIChE J.* (1959) **5**, 384.
11. Paul, E. L., Treybal, R. E., *AIChE J.* (1971) **17**, 718.
12. Saddy, M., Luchi, N. R., *Lat. Am. J. Chem. Eng. Appl. Chem.* (1972) **2**, 3.
13. Renken, A., *Chem. Eng. Sci.* (1972) **27**, 1925.
14. Newberger, M., Kadlec, R. H., *AIChE J.* (1971) **17**, 1381.
15. Ritchie, B. W., Tobgy, A. H., *Chem. Eng. Sci.* (1974) **29**, 533.
16. Tobgy, A. H., Ph.D. Thesis, University of Exeter (1974).
17. Treleaven, C. R., Tobgy, A. H., *Chem. Eng. Sci.* (1973) **28**, 413.
18. Vassilatas, G., Toor, H. L., *AIChE J.* (1965) **11**, 666.
19. Kattan, A., Adler, R. J., *AIChE J.* (1967) **13**, 580.
20. Harris, I. J., Srivastava, R. D., *Can. J. Chem. Eng.* (1968) **46**, 66.
21. Rao, D. P., Dunn, I. J., *Chem. Eng. Sci.* (1970) **25**, 1275.
22. Rao, D. P., Edwards, L. L., *Ind. Eng. Chem., Fundamentals* (1971) **17**, 398.
23. Rao, D. P., Edwards, L. L., *AIChE J.* (1971) **17**, 1264.
24. Evangelista, J. J., Katz, S., Shinnar, R., *AIChE J.* (1969) **15**, 843.
25. Van de Vusse, J. G., *Chem. Eng. Sci.* (1955) **4**, 178, 209.
26. Otte, L. L., *et al.*, *AIChE Ann. Meetg., 64th, San Francisco, Nov. 28, 1971*.
27. Evangelista, J. J., Shinnar, R., Katz, S., *Proc. Symp. (Int.) Combust., 12th*, p. 901, The Combustion Institute (1969).
28. Komazawa, I., Sasakura, T., Otake, T., *Chem. Eng. Japan* (1969) **2**, 208.
29. Villermaux, J., Devillon, J.-C., *Fifth European/Second Intern. Symp. Chem. Reaction Eng., Amsterdam, May 2-4, 1972*, pp. B1-13, Elsevier, Amsterdam (1972).
30. Butcher, J. C., *Austr. Math. Soc. J.* (1964) **4**, 179.
31. Lapidus, L., Seinfeld, J. H., "Numerical Solution of Ordinary Differential Equations," Academic, New York, 1971.
32. Ng, D. Y. C., Rippin, D. W. T., *Proc. European Symp. Chem. Reaction Eng., 3rd, Amsterdam, 1964*, pp. 161, Pergamon, Oxford (1965).
33. Anand, U. S., Ph.D. Thesis, University of London (1967).
34. Harada, M. *et al.*, *Mem. Fac. Eng. Kyoto Univ.* (1962) **24**, 431.
35. Yamazaki, H., Ichikawa, A., *Int. Chem. Eng.* (1970) **10**, 471.
36. Costa, P., Trevissoi, C., *Chem. Eng. Sci.* (1972) **27**, 2041.
37. Ritchie, B. W., Tobgy, A. H., written comment on paper B1-13, *Fifth European/Second Int. Symp. Chem. Reaction Eng., Amsterdam, May 2-4, 1972*.
38. Tobgy, A. H., University of Exeter, *Chem. Eng. Dept. Tech. Rept. No. CRE 5* (1973).
39. Spielman, L. A., Levenspiel, O., *Chem. Eng. Sci.* (1965) **20**, 247.
40. Kattan, A., Adler, R. J., *Chem. Eng. Sci.* (1972) **27**, 1013.
41. Rao, D. P., Edwards, L. L., *Chem. Eng. Sci.* (1973) **28**, 1179.
42. Treleaven, C. R., Tobgy, A. H., *Chem. Eng. Sci.* (1972) **27**, 1653.
43. Ritchie, B. W., Tobgy, A. H., University of Exeter, *Chem. Eng. Dept. Tech. Rept. No. CRE 6* (1973).
44. Novosad, Z., Thyn, J., *Collection Czech. Chem. Commun.* (1966) **31**, 3710.

RECEIVED January 2, 1974.